Postharvest Biology and Technology 233 (2026) 114041

Contents lists available at ScienceDirect

Postharvest Biology and Technology

journal homepage: www.elsevier.com/locate/postharvbio

Etiology of postharvest fungal decay in kumquat: A polyphasic approach integrating aggressiveness, iPBS and SCoT fingerprinting, and multilocus phylogeny

Mehtap Alkan [a], Göksel Özer [a,*], Muharrem Türkkan [b,*], Tuğba Bozoğlu [b], İsmail Erper [c,d], Elif Yıldırım [c], Davut Soner Akgül [e], T. Tarık Erper [e], Rachid Lahlali [f], Sibel Derviş [g,*]

[a] Department of Plant Protection, Faculty of Agriculture, Bolu Abant Izzet Baysal University, Bolu 14030, Türkiye
[b] Department of Plant Protection, Faculty of Agriculture, Ordu University, Ordu 52200, Türkiye
[c] Department of Plant Protection, Faculty of Agriculture, Ondokuz Mayıs University, Samsun 55139, Türkiye
[d] Department of Plant Protection, Faculty of Agriculture, Kyrgyz Turkish Manas University, Bishkek 720044, Kyrgyzstan
[e] Department of Plant Protection, Agriculture Faculty, Çukurova University, Adana 01330, Türkiye
[f] Phytopathology Unit, Department of Plant Protection, Ecole Nationale d'Agriculture de Meknès, BP S/40, Meknès 50000, Morocco
[g] Department of Plant Protection, Faculty of Kızıltepe Agricultural Sciences and Technologies, Mardin Artuklu University, Mardin 47000, Türkiye

ARTICLE INFO

Keywords:
Fortunella margarita
Citrus japonica
Postharvest pathology
Fungal pathogens
Molecular identification
Food spoilage

ABSTRACT

As the global popularity of kumquat (*Fortunella* spp.; syn. *Citrus japonica*) continues to rise, knowledge of the pathogens responsible for postharvest losses remains limited. This study presents the first etiological investigation of postharvest fungal decay in kumquat, using a multi-regional survey and polyphasic characterization. A pathogenic complex responsible for postharvest decay was identified on this host for the first time, consisting of *Alternaria alternata* ($n = 23$), *Geotrichum citri-aurantii* ($n = 17$), *Penicillium digitatum* ($n = 30$), *P. italicum* ($n = 8$), and *P. expansum* ($n = 4$). Identification combined morphological characterization with high-resolution molecular fingerprinting using start codon targeted (SCoT 32) and inter-primer binding site (iPBS 2395) markers, yielding polymorphic profiles that provided clear species-level discrimination consistent with multilocus phylogenetic analysis. *In vitro* assays identified distinct thermal optima for each pathogen. *Geotrichum citri-aurantii* growth was maximal at 30 °C, whereas *P. expansum* grew optimally at 20 °C. The remaining species–*P. digitatum*, *P. italicum*, and *A. alternata*–all achieved maximum growth at 25 °C, although *P. italicum* demonstrated a broad optimal range spanning from 20 to 25 °C. Aggressiveness varied among the pathogens, with *P. digitatum* and *A. alternata* being the most aggressive, followed by *G. citri-aurantii* and *P. expansum*, while *P. italicum* was the least aggressive. This study establishes the first pathogenic profile for kumquat decay, providing a framework for evidence-based postharvest management. The demonstrated efficiency of SCoT 32 and iPBS 2395 markers highlights their value as powerful, rapid, and cost-effective tools for pathogen surveillance and taxonomic resolution in postharvest pathology.

1. Introduction

The Nagami kumquat (*Fortunella margarita* [Lour.] Swingle; syn. *Citrus japonica*) has carved out an expanding niche in global markets, valued for its distinctive flavor and dense nutritional profile of dietary fiber, vitamins, and bioactive compounds (Pawełczyk et al., 2023; Fernandes et al., 2025). Its primary appeal is inextricably linked to its greatest vulnerability: unlike most citrus, it is consumed whole, a practice that enhances its antioxidant properties but also magnifies its susceptibility to surface-colonizing pathogens (Wu et al., 2018; Chai et al., 2022). This risk is compounded by a thin pericarp that offers minimal protection against water loss and microbial invasion, creating significant postharvest challenges (Schirra et al., 2011). Although various strategies have been explored to mitigate these losses–from physical methods such as hot water soaking (Schirra et al., 2011) and cuticular wax modulation (Yang et al., 2022, 2023) to the use of natural

* Corresponding authors.
E-mail addresses: ozer_g@ibu.edu.tr (G. Özer), muharremturkkan@odu.edu.tr (M. Türkkan), sibeldervis@artuklu.edu.tr (S. Derviş).

https://doi.org/10.1016/j.postharvbio.2025.114041
Received 20 September 2025; Received in revised form 24 October 2025; Accepted 30 October 2025
Available online 3 November 2025
0925-5214/© 2025 Elsevier B.V. All rights are reserved, including those for text and data mining, AI training, and similar technologies.

antioxidants such as ellagic acid (Liu et al., 2018)–these approaches often focus on mitigating decay symptoms without a clear understanding of specific etiological factors. Even recent studies on single cultivars such as the 'Huapi' mutant, which linked improved storage performance to epicuticular wax and flavonoid metabolism, highlight the biological basis of susceptibility without identifying the primary pathogen invasion (Ma et al., 2021; Zhu et al., 2024).

This gap in understanding postharvest pathogens contrasts sharply with the extensive knowledge of kumquat diseases in the field. Agronomic research has identified the causal agents of major pre-harvest diseases, including twig dieback (*Colletotrichum karsti*, *Diaporthe* spp.), trunk canker (*Lasiodiplodia theobromae*), root rot (*Phytophthora cinnamomi*), and various shoot cankers and blights (*Fusarium* spp., *Phytophthora citrophthora*) (Guarnaccia and Crous, 2017; Gui et al., 2020; Jung et al., 2016; Kurbetli et al., 2016; Leonardi et al., 2023; Zhu et al., 2013). However, this detailed pre-harvest knowledge creates a scientific blind spot around the postharvest supply chain, where significant economic losses manifest. For major citrus crops, this phase is well understood; decay is driven by a destructive and well-defined pathogen complex. This includes *Alternaria alternata*, which causes black rot originating from latent infections (Peever et al., 2004; Güney et al., 2023), the economically dominant molds *Penicillium digitatum* and *P. italicum*, and the opportunistic *P. expansum* (Cheng et al., 2020; Kanashiro et al., 2020). Compounding these threats is the aggressive sour rot agent, *G. citri-aurantii*, known for its rapid spread and increasing fungicide resistance (Saito and Xiao, 2017; Ai et al., 2025; Nguyen et al., 2025). While this suite of pathogens is well-characterized in other citrus, its role in kumquat decay remains entirely unestablished.

To bridge this knowledge gap effectively, a modern polyphasic framework that integrates classical morphology with high-resolution molecular tools is essential. While multilocus sequence analysis (MLSA) remains the gold standard for phylogenetic resolution, its application to large isolate collections is often constrained by cost and labor. Therefore, we adopted a tiered strategy, first employing retrotransposon-based inter-primer binding site (iPBS) and gene-based start-codon targeted (SCoT) markers. These techniques are increasingly utilized for their power in providing precise species delineation and epidemiological inference across diverse fungal systems (Collard and Mackill, 2009; Kalendar et al., 2010; Aydın et al., 2020, 2022; Palacıoğlu et al., 2023; Tekin et al., 2024; Türkkan et al., 2024; Muratali et al., 2025). This initial high-throughput screening allows for robust grouping of isolates, with representative strains then subjected to confirmatory MLSA to ensure accurate phylogenetic placement and linkage to ex-type reference strains.

Based on the established pathogenic profile of major citrus crops, we hypothesized that the postharvest decay observed in commercial kumquats is caused by the same, or a very similar, complex of fungal pathogens. The primary aim of this investigation was, therefore, to conduct the first comprehensive etiological study of postharvest fungal decay in kumquat. Using the robust polyphasic approach outlined above, we sought to: (1) isolate and identify the fungal pathogens from symptomatic kumquat fruit sourced from commercial markets; (2) confirm species-level identities using a combination of morphological characterization, iPBS/SCoT molecular fingerprinting, and MLSA; and (3) characterize the aggressiveness and thermal biology of the identified pathogens through *in vivo* pathogenicity trials that fulfill Koch's postulates. This comprehensive approach was designed to rigorously test our hypothesis and establish the foundational pathogenic profile necessary for developing targeted and effective postharvest management strategies.

2. Material and methods

2.1. Sampling, isolation, and morphological characterization

Nagami kumquat, cultivated almost exclusively in the Mediterranean region of Türkiye, with major production centered in Antalya and Mersin, is widely distributed through national market chains. To capture the diversity of postharvest pathogens under retail market conditions, a purposive multi-stage sampling survey was conducted in 2025. The survey covered five provinces selected from three distinct geographical regions: Ankara (Central Anatolia), Mardin (Southeastern Anatolia), and three provinces representing the breadth of the Black Sea region–Bolu (western), Samsun (central), and Ordu (eastern). Within each province, samples were collected from 4 to 5 different retail markets, including supermarkets and local fruit vendors, for a total of 23 retail locations. Because kumquats are almost exclusively marketed in sealed clamshell plastic containers, symptomatic fruit were sampled directly from these packages to ensure that decay reflected natural retail conditions. To avoid pseudoreplication, only one representative symptomatic fruit was collected per container. In total, 82 symptomatic fruit exhibiting postharvest decay symptoms (e.g., soft rot, sunken lesions, visible mold growth, peel discoloration) were collected. Each fruit was aseptically removed from its clamshell, placed in an individual sterile polyethylene bag, transported in cooled insulated containers, and processed within 24 h. Fungi were isolated from lesion margins on potato dextrose agar (PDA; Merck, Germany), and representative colonies were subcultured to obtain pure isolates for morphological, molecular, and pathogenic characterization.

For fungal isolation, 5 × 5 mm tissue segments were excised from the advancing margin of lesions, surface-disinfested in 1 % NaOCl (1 min), rinsed twice with sterile distilled water, and blotted dry. Tissues were plated on PDA supplemented with 50 mg L^{-1} streptomycin sulfate and incubated in darkness at 25 ± 1 °C for 5–7 d. Axenic cultures were obtained by transferring hyphal tips or single spores to fresh PDA.

Isolates were preliminarily identified using cultural and morphological traits. Colony color, texture, and growth habit were recorded, and representative *Alternaria* isolates were grown on multiple diagnostic media (Oatmeal Agar, Corn Meal Agar, V8 Juice Agar, and Synthetic Nutrient-Poor Agar) to assess zonation and pigmentation. Microscopic features were examined in water mounts: *Alternaria* was recognized by dark mycelia and chains of muriform conidia (Simmons, 2007); *Geotrichum* by white yeast-like colonies and fragmenting hyphae producing arthroconidia (de Hoog et al., 1986); and *Penicillium* spp. by conidiophore branching, phialide morphology, and colony coloration (Frisvad and Samson, 2004).

2.2. Genetic diversity analysis using iPBS and SCoT markers

Mycelial cultures of representative isolates were grown on PDA at 25 °C for 7 d prior to DNA extraction. Approximately 100 mg of fresh mycelium was scraped aseptically from the colony surface, frozen in liquid nitrogen, and homogenized with a sterile micropestle. Genomic DNA was extracted using the DNeasy Plant Mini Kit (Qiagen, Hilden, Germany) following the manufacturer's protocol, and extracts were stored at –20 °C until use.

To assess the genetic diversity of the fungal population and to guide the selection of representative isolates for MLSA, we employed two molecular fingerprinting techniques: retrotransposon-based inter-primer binding site (iPBS) and start-codon-targeted (SCoT) analysis. The analysis was performed using primers SCoT 32 and iPBS 2395, following the detailed PCR and electrophoresis protocols described by Gültekin et al. (2025) and Muratali et al. (2025), respectively. Reproducible banding patterns were scored to generate a binary matrix. Similarity matrices were generated independently for both iPBS and SCoT datasets using Jaccard's coefficient. The congruence between the two marker systems was then evaluated by performing a Mantel test to calculate the correlation between these two matrices using the NTSYS–pc v2.02 software (Rohlf, 2000). Given the high correlation, the binary data from both markers were combined to generate a single, more robust UPGMA dendrogram for the final analysis.

2.3. Multilocus sequencing and phylogenetic analysis

To confirm species identity and determine phylogenetic relationships, multilocus sequence analysis (MLSA) was performed on a selection of representative isolates. For each of the five fungal species, two to three isolates were selected as representatives based on two criteria: (1) their position within distinct genetic clusters identified by iPBS/SCoT analysis, ensuring coverage of intraspecific genetic diversity, and (2) their geographic origin, to capture spatial variation. This selection strategy prioritized genetic representativeness rather than pathogenicity levels, as the primary goal was to confirm species identity across the full diversity of recovered isolates.

The selection of gene regions for amplification was guided by their established taxonomic utility for each genus. For *Alternaria*, the Internal Transcribed Spacer (ITS), translation elongation factor 1-alpha (*tef1-α*), RNA polymerase II second largest subunit (*rpb2*), *Alternaria alternata* major allergen 1 gene (*Alt-a1*), and glyceraldehyde-3-phosphate dehydrogenase (*gpd*) genes were amplified using primers and conditions adapted from Woudenberg et al. (2015). For *Geotrichum*, the ITS and Large Subunit (LSU) regions (of ribosomal RNA) were targeted following the protocol described by Zhu et al. (2024). Finally, for *Penicillium*, beta-tubulin (*BenA*), calmodulin (*CaM*), and *rpb2* genes were amplified with primers and conditions as defined by Houbraken et al. (2016). We purified all successfully amplified PCR products and sent them to BMLabosis (Ankara, Türkiye) for bidirectional Sanger sequencing.

After sequencing, raw chromatograms were inspected in FinchTV v1.4.0, assembled the high-quality reads into consensus sequences, and performed alignments using the MAFFT algorithm. Species identities were then validated through BLASTn comparisons against authenticated reference strains from the GenBank database.

Phylogenetic relationships were inferred from individual and concatenated multilocus datasets using the Maximum Likelihood (ML) method. ML analysis was performed via the CIPRES Science Gateway portal (Miller et al., 2011) using IQ-Tree software (Nguyen et al., 2025). The optimal nucleotide substitution models were determined according to the Akaike information criterion. Statistical support for branching patterns was assessed by 1000 ultrafast bootstrap replicates, with values below 70 % not displayed. *Talaromyces flavus* (CBS 310.38), *Alternaria alternantherae* (CBS 124392), and *Magnusiomyces capitatus* (CBS 162.80) served as outgroups for *Penicillium*, *Alternaria*, and *Geotrichum* phylogenies, respectively. Final trees were visualized and edited for publication using FigTree v1.4.4 and MEGA X software (Kumar et al., 2018).

2.4. Effect of temperature on mycelial growth

The effect of temperature on *in vitro* mycelial growth was assessed using a specific panel of ten isolates. The isolates for *A. alternata*, *G. citri-aurantii*, *P. expansum*, and *P. italicum* were identical to those used for MLSA. For *P. digitatum*, two of the three isolates from the MLSA, MaCjPd01 and OrCjPd01, were selected for this and subsequent assays. Mycelial plugs (5 mm^2) taken from the actively growing margins of 5-day-old PDA cultures were placed at the center of 90-mm Petri dishes containing 15 ML PDA. Plates were incubated in darkness for 7 d at constant temperatures ranging from 5 to 40 °C at 5 °C intervals. Colony diameter was measured along two perpendicular axes, and mean values were used to calculate daily radial growth rates (mm d^{-1}). The experiment was conducted twice, each run including four replicates per isolate–temperature combination.

2.5. Pathogenicity and aggressiveness assays

To fulfill Koch's postulates, the pathogenicity of the identical set of ten isolates used in the mycelial growth experiments was evaluated on healthy kumquat fruit (*Fortunella margarita* cv. Nagami). Fruit of uniform size and maturity, free of defects, were surface-disinfested by immersion in 1 % NaOCl for 40 s and 70 % ethanol for 60 s, rinsed three times with sterile distilled water, and air-dried under laminar flow. Inocula were prepared as 1×10^6 conidia ML^{-1} suspensions from 7-day-old cultures of *A. alternata* and *Penicillium* spp. For *G. citri-aurantii*, a 1×10^6 arthroconidia ML^{-1} suspension was obtained by scraping and homogenizing 7-day-old cultures in sterile water. Fruit were wounded with a sterile pipette tip to a depth of 2 mm, with inoculation sites adjusted according to pathogen ecology: *A. alternata* was inoculated at the stem-end, reflecting its frequent association with stem-end tissues, while *P. digitatum*, *P. italicum*, *P. expansum*, and *G. citri-aurantii* were inoculated at the equatorial region. A 10 μL aliquot of the respective inoculum was deposited into each wound. Control fruit were treated identically but inoculated with sterile water. The assay was conducted twice, each trial comprising six replicates fruit per isolate. Inoculated fruit were placed in sterile containers with moistened filter paper, incubated at 25 °C for 7 d, and assessed for symptom development. Lesion areas (cm^2) were measured with ImageJ software (version 1.53i, National Institutes of Health, USA).

2.6. Statistical analysis

Data from *in vitro* temperature–growth assays (daily radial growth rate, mm d^{-1}, calculated from mean colony diameters measured along two axes) and *in vivo* pathogenicity assays (lesion area, cm^2) were analyzed. To satisfy parametric assumptions, values were Box–Cox transformed ($k + 1$). Treatment effects were tested by one-way ANOVA, and significant differences among means were determined using Tukey's HSD at $P < 0.05$. All analyses were performed with XLSTAT (version 2016.02.28451, Addinsoft, USA).

3. Results

3.1. Symptom observation and fungal isolation

From the surveys, 82 kumquat fruit exhibiting postharvest decay were collected, each originating from a distinct retail package. The prohibitive retail cost precluded a quantitative assessment of market-wide disease incidence; however, symptomatic containers were readily encountered. It was consistently observed that affected fruit from the same container all exhibited the same type of decay. The collective symptoms documented across all containers included watery soft rot, sunken lesions, peel discoloration, and conspicuous sporulation in white, cream, green, blue, or black hues (Fig. 1). Pathogenicity testing attributed these symptoms to five principal rot types: black rot caused by *A. alternata*, sour rot caused by *G. citri-aurantii*, green mold caused by *P. digitatum*, and two forms of blue mold caused by *P. italicum* and *P. expansum*. From lesion margins, a total of 82 fungal isolates were recovered, purified, and maintained for downstream analyses. The species distribution was as follows: *A. alternata* was represented by 23 isolates from Ankara and Bolu; *G. citri-aurantii* by 17 isolates exclusively from Ankara; *P. digitatum* by 30 isolates from Ankara, Mardin, Ordu, and Samsun; *P. expansum* by 4 isolates from Ankara; and *P. italicum* by 8 isolates from Bolu and Ordu. Notably, *A. alternata* was most frequently associated with stem-end tissues, where quiescent infections likely initiated during flowering or early fruit development and later manifested postharvest as black rot lesions.

3.2. Cultural and morphological characterization

Following purification, all 82 fungal isolates were identified to species level based on their distinct macroscopic and microscopic features (Fig. 2). A pathogenic complex of five species across three genera was recovered. Twenty-three isolates were identified as *A. alternata*. On PDA, colonies grew rapidly, developing a dense, cottony texture that matured from grayish-white to dark olivaceous-green or sooty black, consistently producing a bright yellow to ochre diffusible pigment on the reverse. Colony morphology varied considerably with medium: on PDA and



Fig. 1. Typical symptoms of postharvest fungal decay observed on commercially sold kumquat (*Fortunella margarita*) fruit. (A, B) Symptoms of black rot showing dark sporulation characteristic of *Alternaria* spp.; (C) A sunken lesion typical of sour rot caused by *Geotrichum* spp.; (D-F) Green and blue mold development, characterized by white mycelia and colored sporulation, caused by *Penicillium* spp.

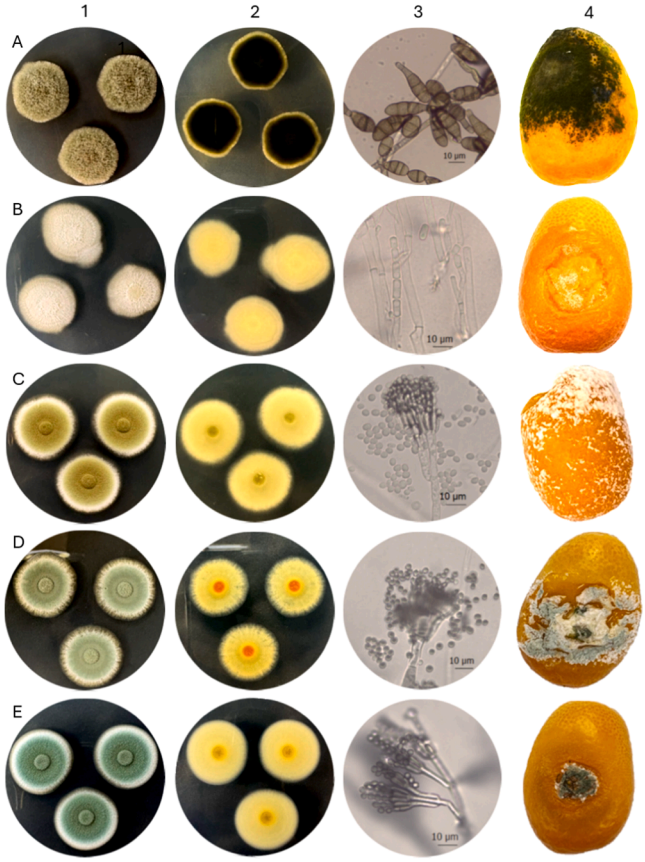


Fig. 2. Morphological, cultural, and pathogenic characteristics of five fungal pathogens isolated from kumquat. Each row corresponds to a different species: (A) *Alternaria alternata*, (B) *Geotrichum citri-aurantii*, (C) *Penicillium digitatum*, (D) *P. italicum*, and (E) *P. expansum*. Columns represent: (1) colony morphology on PDA, (2) colony reverse, (3) microscopic structures (scale bars = 10 µm), and (4) symptoms on wounded *Fortunella margarita* fruit at 7 d post inoculation, 25 °C. Diagnostic features include the olivaceous-green colony and muriform conidia of *A. alternata* causing dark mycelial growth and soft rot; the white, yeast-like colony and cylindrical arthroconidia of *G. citri-aurantii* causing sour rot; the olive-green colony and cylindrical conidia of *P. digitatum* causing green mold; the blue-green colony and globose conidia of *P. italicum* causing blue mold; and the dull blue-green tufted colony and globose conidia of *P. expansum* causing blue-green mold with soft rot.

OAT, isolates were dense and fast-growing with dark pigmentation and velvety to cottony textures; on CMA, colonies were paler and floccose, lacking reverse pigmentation; on V8, growth was sparse and appressed but displayed distinct concentric zonation; and on SNA, colonies were restricted and largely submerged, forming translucent mycelia that facilitated direct microscopic observation. Microscopically, the isolates showed septate, brown hyphae and acropetal chains of brown, muriform conidia measuring 18–40 × 8–16 µm (n = 40 conidia).

Seventeen isolates were identified as *G. citri-aurantii*. Colonies were flat, white to cream, yeast-like, with a dry, powdery surface and a characteristic sour odor. Microscopic examination revealed hyaline, septate hyphae that fragmented into cylindrical to barrel-shaped arthroconidia measuring 4–12 × 3–6 µm (n = 30 conidia).

The remaining 42 isolates belonged to *Penicillium* and were divided into three species. *Penicillium digitatum* was the most common, represented by thirty isolates, producing fast-spreading, velvety olive-green colonies with prominent white margins. Terverticillate conidiophores generated long chains of smooth-walled, cylindrical to ellipsoidal conidia measuring 4.5–11 × 3–8 µm (n = 50 conidia). Eight isolates were identified as *P. italicum*, which exhibited more restricted growth, blue-green to grayish sporulation, and irregularly branched terverticillate conidiophores bearing disordered chains of smooth, globose to subglobose conidia measuring 3–5 × 2.5–4.5 µm (n = 40 conidia). The final four isolates were identified as *P. expansum*, which produced dull blue-green, tufted colonies that aged to grayish-brown and were distinguished by robust conidiophores and compact columnar chains of globose, smooth-walled conidia measuring 3–4 µm in diameter (n = 35 conidia).

3.3. Genetic diversity analysis using iPBS and SCoT markers

Genetic diversity analysis using iPBS and SCoT markers produced highly polymorphic and reproducible DNA fingerprints for all 82 fungal isolates, demonstrating the effectiveness of this approach (Fig. 3). Collectively, the two primers generated 35 scorable bands, of which 33 (94.3 %) were polymorphic, indicating a high level of genetic diversity. The SCoT 32 primer was slightly more informative, yielding 19 bands with a resolving power (RP) of 8.63, compared to the iPBS 2395 primer, which produced 16 bands with an RP of 7.76. Both markers showed strong discriminatory capacity, reflected by an identical Polymorphism Information Content (PIC) of 0.31.

The Mantel test revealed a very high and significant correlation between the similarity matrices generated from the iPBS and SCoT markers (r = 0.92), indicating a strong congruence between the two datasets.

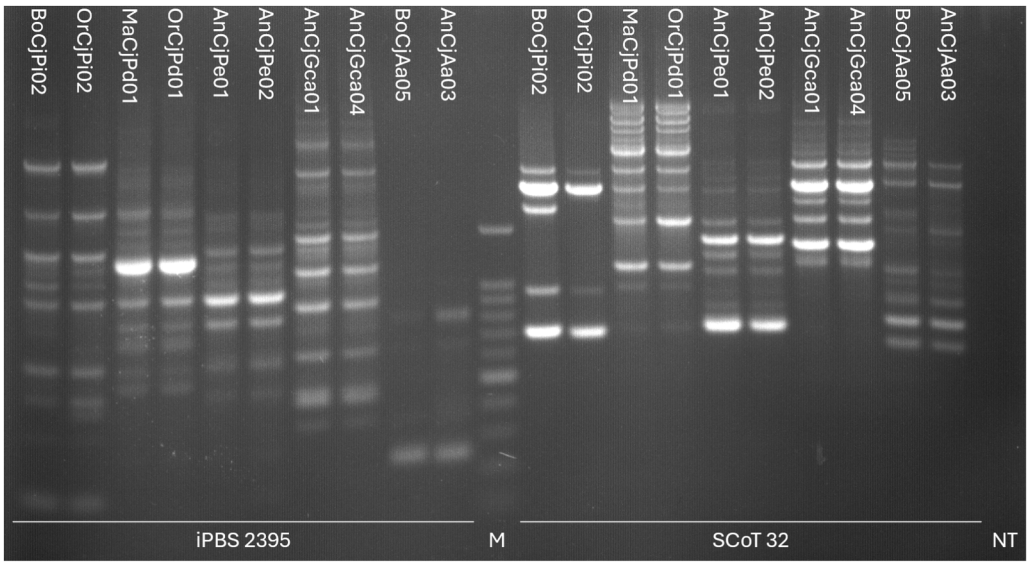


Fig. 3. Molecular fingerprinting profiles demonstrating species-level discrimination among kumquat fungal pathogens using iPBS 2395 and SCoT 32 markers. Representative DNA banding patterns generated by iPBS 2395 (left panel) and SCoT 32 (right panel) primers for selected isolates from each of the five fungal species. Lane M: 100 bp DNA Ladder (Solis BioDyne, Tartu, Estonia). NT: No template control. Isolate codes indicate species and geographic origin: An = Ankara, Bo = Bolu, Ma = Mardin, Or = Ordu, Sa = Samsun; Cj = *Citrus japonica* (kumquat); Aa = *Alternaria alternata*, Gca = *Geotrichum citri-aurantii*, Pd = *Penicillium digitatum*, Pe = *P. expansum*, Pi = *P. italicum*.

Therefore, a combined analysis was performed to construct a single dendrogram. The combined iPBS and SCoT data resolved the 82 fungal isolates into five distinct and well-supported genetic clusters that perfectly corresponded with the five identified species.

Intraspecific genetic diversity was limited across all five species, with no evidence of geographic clustering, suggesting pathogen dispersal primarily via commercial distribution networks rather than regional differentiation.

3.4. Phylogenetic confirmation of species identity

Multilocus sequence analysis unequivocally confirmed the species identity of all representative isolates. Intraspecific sequence conservation was high, with ITS and *BenA* loci showing 100 % identity within each species. Similarly, *CaM* and *rpb2* sequences shared > 99 % identity with their respective ex-type or authenticated reference strains in GenBank.

Reflecting these high sequence similarities, all phylogenetic analyses consistently resolved the five species into distinct, strongly supported monophyletic clades with their corresponding type strains (bootstrap support ≥95 %; Fig. 4). Specifically, *G. citri-aurantii* isolates clustered with type strains CBS 175.89^{T} and CBS 176.89^{T} (Fig. 4A), and *A. alternata* isolates clustered with type strains CBS 916.96^{T} and CBS 119399 (Fig. 4B). Likewise, isolates of *P. expansum*, *P. italicum*, and *P. digitatum* grouped respectively with their type strains CBS 325.48^{T}, CBS 339.48^{T}, and CBS 112082^{T}, clustering within the *Fasciculata* and *Penicillium* sections (Fig. 4C). Notably, the phylogenetic clustering derived from this MLSA was fully congruent with the genetic groups previously identified using iPBS and SCoT markers.

3.5. Effect of temperature on mycelial growth

The mycelial growth of all five species was significantly influenced by temperature, revealing distinct performance profiles for each pathogen ($P < 0.05$) (Table 1). *Penicillium expansum* growth was statistically highest at 20 °C, decreased significantly at 25 °C, and ceased entirely at 35 °C. In contrast, the growth of *G. citri-aurantii* steadily increased with temperature to reach a statistically significant maximum at 30 °C, a point where the growth of most other species had already declined. The remaining three species all achieved their maximum growth at 25 °C but were distinguished by their performance across other temperatures. Both *P. digitatum* and *A. alternata* displayed sharp optima, as their growth decreased significantly at temperatures immediately above and below 25 °C. However, *A. alternata* was able to grow across the entire temperature span tested (5–40 °C), while *P. digitatum* growth ceased above 35 °C. Different from these sharp peaks, *P. italicum* maintained statistically equivalent high growth at both 20 °C and 25 °C before its growth also ceased at 35 °C.

3.6. Pathogenicity and aggressiveness assays

All representative isolates of the five species were confirmed to be pathogenic on wounded kumquats, inducing distinct decay symptoms and fulfilling Koch's postulates, while control fruit remained symptomless (Fig. 2). After seven days at 25 °C, *A. alternata* caused a firm, spreading dark brown to black rot, and *G. citri-aurantii* produced a characteristic sour rot with watery lesions and a cream-colored, yeast-like slime. The *Penicillium* species induced moldy rots differentiated by their sporulation: *P. digitatum* generated an extensive green mold leading to fruit mummification, whereas *P. italicum* and *P. expansum* caused typical blue and blue-green molds, respectively.

Beyond these symptomatic differences, the quantitative aggressiveness, measured by lesion area, also varied significantly among the pathogens (Fig. 5; ANOVA: $F(9, 110) = 5.955$, $P < 0.0001$). *Penicillium digitatum* and *A. alternata* isolates were the most virulent, consistently producing the largest lesions with mean areas ranging from 6.41 to 7.12 cm^2. Conversely, *P. italicum* was identified as the least aggressive pathogen, causing significantly smaller lesions with a mean area of approximately 5.10 cm^2. The aggressiveness of *G. citri-aurantii* and *P. expansum* was intermediate, as the lesions they caused were not statistically different from those of the most aggressive species, nor did they differ significantly from the smallest lesions caused by the least aggressive *P. italicum*.

4. Discussion

This study provides the first comprehensive etiological map of postharvest fungal decay in commercially marketed kumquats,

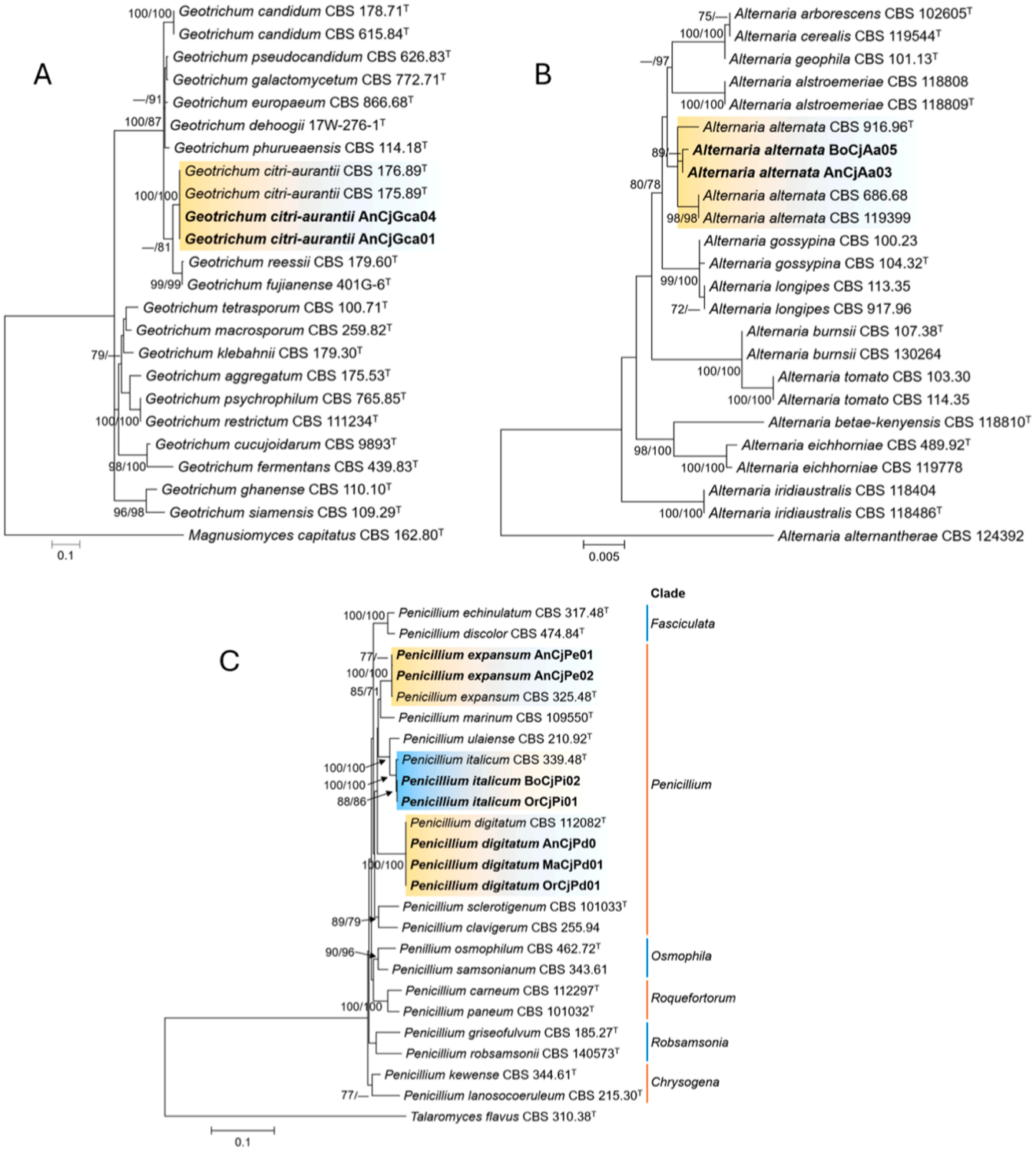


Fig. 4. Maximum Likelihood phylogenetic trees based on combined sequences, illustrating the relationships of fungal isolates from kumquat with reference and type strains. (A) The tree for *Geotrichum citri-aurantii* resolves the isolates into a distinct monophyletic lineage with the type strains CBS 175.89^{T} and CBS 176.89^{T}, using *Magnusiomyces capitatus* CBS 162.80^{T} as the outgroup. (B) The tree for *Alternaria alternata* clusters the isolates tightly with the type strains CBS 916.96^{T} and CBS 119399^{T}, using *Alternaria alternantherae* CBS 124392^{T} as the outgroup. (C) The tree for *Penicillium* resolves isolates of *P. expansum* (CBS 325.48^{T}), *P. italicum* (CBS 339.48^{T}), and *P. digitatum* (CBS 112082^{T}) into distinct, well-supported clades, using *Talaromyces flavus* CBS 310.38^{T} as the outgroup. Bootstrap support values from ML and Maximum Parsimony (MP) analyses Bootstrap values $\geq$ 70 % (from 1000 replicates) are indicated at the nodes (ML/MP). The isolates from this study are shown in bold.

Table 1
Characteristics of isolates, molecular markers, pathogenicity, and growth rate profiles of five fungal species associated with kumquat postharvest decay.

Category	Locus Trait	*Alternaria alternata*	*Geotrichum citri-aurantii*	*Penicillium digitatum*	*Penicillium expansum*	*Penicillium italicum*
Location(s)		Ankara Bolu	Ankara	Ankara Mardin Ordu Samsun	Ankara	Bolu Ordu
Total number of isolates		23	17	30	4	8
SCoT clade assignment		c	d	a	e	b
iPBS clade assignment		c	d	a	e	b
Representative isolates		AnCjAa03 BoCjAa05	AnCjGca01 AnCjGca04	AnCjPd02* MaCjPd01 OrCjPd01	AnCjPe01 AnCjPe02	BoCjPi02 OrCjPi01
GenBank accession numbers**	**ITS**	PX279250 PX279251	PX279252 PX279253	–	–	–
	LSU	PX289805 PX289806	PX279257 PX279258	–	–	–
	tef1-α	PX289811 PX289812	–	–	–	–
	Alt-a1	PX289809 PX289810	–	–	–	–
	gpdh	PX289807 PX289808	–	–	–	–
	rpb2	–	–	PX289819 PX289820 PX289821	PX289826 PX289827	PX289832 PX289833
	BenA	–	–	PX289813 PX289814 PX289815	PX289822 PX289823	PX289828 PX289829
	CaM	–	–	PX289816 PX289817 PX289818	PX289824 PX289825	PX289830 PX289831
Mean radial growth rate (mm d^{-1})***	5 °C	1.34 ± 0.03 e 1.37 ± 0.01 e	1.81 ± 0.04 h 1.80 ± 0.02 h	2.69 ± 0.06 f 2.71 ± 0.03 f	2.39 ± 0.06 d 2.34 ± 0.03 d	1.30 ± 0.04 d 1.31 ± 0.02 d
	10 °C	2.10 ± 0.07 d 2.09 ± 0.04 d	2.31 ± 0.06 g 2.30 ± 0.04 g	3.81 ± 0.07 de 3.78 ± 0.03 e	3.05 ± 0.06c 3.07 ± 0.03c	2.40 ± 0.07c 2.41 ± 0.03c
	15 °C	3.11 ± 0.05c 3.08 ± 0.01c	3.31 ± 0.10 e 3.30 ± 0.05 e	5.13 ± 0.11c 5.23 ± 0.07c	3.93 ± 0.08 b 3.88 ± 0.04 b	3.01 ± 0.04 b 3.06 ± 0.01 b
	20 °C	3.65 ± 0.06 b 3.63 ± 0.03 b	4.58 ± 0.05 d 4.60 ± 0.02 d	6.38 ± 0.12 b 6.40 ± 0.06 b	4.26 ± 0.06 a 4.27 ± 0.03 a	3.53 ± 0.07 a 3.49 ± 0.04 a
	25 °C	4.24 ± 0.13 a 4.26 ± 0.08 a	5.20 ± 0.09 bc 5.13 ± 0.03c	6.95 ± 0.10 a 6.98 ± 0.05 a	3.78 ± 0.06 b 3.76 ± 0.03 b	3.70 ± 0.06 a 3.67 ± 0.03 a
	30 °C	2.86 ± 0.04c 2.85 ± 0.02 c	5.50 ± 0.07 a 5.46 ± 0.03 ab	4.05 ± 0.06 de 4.09 ± 0.02 d	1.23 ± 0.05 e 1.19 ± 0.02 e	2.83 ± 0.06 b 2.86 ± 0.02 b
	35 °C	1.31 ± 0.04 e 1.36 ± 0.02 e	2.69 ± 0.04 f 2.73 ± 0.02 f	0.03 ± 0.02 g 0.03 ± 0.02 g	0.00 ± 0.00 f 0.00 ± 0.00 f	0.00 ± 0.00 e 0.00 ± 0.00 e
	40 °C	0.05 ± 0.02 f 0.05 ± 0.02 f	0.03 ± 0.02 i 0.03 ± 0.02 i	0.00 ± 0.00 g 0.00 ± 0.00 g	0.00 ± 0.00 f 0.00 ± 0.00 f	0.00 ± 0.00 e 0.00 ± 0.00 e

*In the experiments on the effect of temperature on mycelial growth, the isolate AnCjPd02 was not included.
**A dash (–) indicates that no sequence data were available for that locus.
***Values represent the mean ± standard error. Temperature–growth assays were conducted twice, each run including four replicates per isolate–temperature combination. For radial growth data, means within each column followed by the same letter are not significantly different according to Tukey's HSD test ($P < 0.05$).

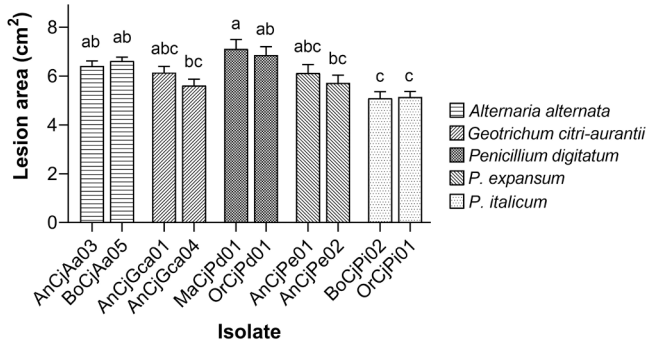


Fig. 5. Aggressiveness of ten fungal isolates from five postharvest pathogen species on kumquat fruit. Bars represent the mean lesion area (cm^2) ± standard error (SE) after seven days of incubation at 25 °C. Different letters above the bars indicate statistically significant differences according to Tukey's HSD test ($P < 0.05$).

fundamentally shifting our understanding of the challenges facing this increasingly popular fruit. By identifying a pathogenic complex comprising *A. alternata*, *G. citri-aurantii*, and three distinct *Penicillium* species (*P. digitatum*, *P. italicum*, *P. expansum*), we have moved beyond artificial inoculations (Guo et al., 2021; Zhu et al., 2024) to confirm their natural occurrence and causal role within the commercial supply chain. The documentation of this complete suite of pathogens on *F. margarita* establishes a critical baseline, directly addressing a knowledge gap that has hindered the development of targeted management strategies for a crop valued for its unique organoleptic and nutritional qualities (Pawełczyk et al., 2023; Fernandes et al., 2025).

A central finding of our investigation is the inextricable link between the kumquat's unique postharvest handling and its susceptibility to this fungal complex. Unlike most citrus, kumquats are retailed almost exclusively in sealed clamshell containers. The high incidence of decay in commercially packaged kumquats presents a paradox. While the packaging prevents mechanical injury, it simultaneously creates a high-humidity, low-ventilation microenvironment that acts as an incubator for fungal pathogens. As our survey design involved sampling fruit produced in Mediterranean hubs from distant retail markets in Central Anatolia, Southeastern Anatolia, and the Black Sea region, long-distance transport is inherent to the supply chain. The ambient temperatures (25–30 °C) likely encountered during such transport delays create ideal conditions for the proliferation of species like *P. digitatum* and *G. citri-aurantii*. This is consistent with the known ecological requirements for postharvest citrus pathogens, including *P. digitatum*, *P. italicum*, and *G. candidum* (Plaza et al., 2003). This phenomenon, where packaging

exacerbates decay, has been well-documented in other delicate commodities like strawberries (Laurin et al., 2005) and pears (Thompson et al., 2008). In kumquats, this issue is critically amplified by the fruit's biology–its thin pericarp offers a weak physical barrier, and its consumption whole means that surface contamination and mycotoxin production, particularly the risk of patulin from *P. expansum* (Chen et al., 2022), pose a direct food safety concern that is less pronounced in peeled citrus.

Methodologically, this study underscores the value of a tiered diagnostic framework for pathogen surveillance within taxonomically complex fungal genera. Morphological criteria alone are notoriously unreliable for discriminating species in *Penicillium* and *Alternaria* (Frisvad and Samson, 2004; Simmons, 2007). Although MLSA remains the gold standard for definitive identification, its cost and labor demands limit its practicality for large-scale screening. Here, the integration of cost-effective iPBS and SCoT fingerprinting provided a powerful, scalable alternative. The strong concordance between fingerprint-based clustering and MLSA outcomes confirms the robustness and diagnostic accuracy of this polyphasic approach. This validation highlights a key operational advantage: the molecular markers deliver reliable species-level resolution, enabling high-throughput surveillance while reserving sequencing for representative isolates. The broader applicability of these marker systems is well supported by previous studies. iPBS markers have successfully revealed genetic diversity in *Cryphonectria parasitica* (Çakar et al., 2023), *Saccharomyces cerevisiae* (Aydın et al., 2022), and several plant-pathogenic fungi (Gültekin et al., 2025; Muratali et al., 2025). Similarly, SCoT markers have proven valuable for resolving fungal phylogenies (Palacıoğlu et al., 2023), detecting intraspecific variation in *Armillaria* spp. (Türkkan et al., 2024), and assessing broader microbial diversity (Tekin et al., 2024). Collectively, these findings and the present results reinforce the versatility and cross-taxonomic reliability of both marker systems.

Beyond species delineation, iPBS and SCoT fingerprints revealed limited intraspecific genetic diversity among all five pathogens examined. The absence of geographic structuring across widely separated provinces spanning roughly 1000 km, coupled with high within-species similarity, suggests recent pathogen introduction and rapid dissemination through national commercial distribution networks rather than long-term regional differentiation. Such genetic homogeneity likely reflects clonal propagation and frequent inter-regional mixing of inoculum via postharvest trade. Nonetheless, continued genomic surveillance remains essential to detect emergent diversity that could underline adaptive shifts in fungicide tolerance or virulence potential.

Our *in vitro* and *in vivo* assays established the distinct ecological roles and threat levels of each pathogen. The high aggressiveness of *P. digitatum*, alongside *A. alternata*, is consistent with their roles as highly destructive postharvest pathogens of citrus worldwide (Cheng et al., 2020). Furthermore, our finding that *A. alternata* primarily caused stem-end rot strongly suggests these infections may begin as latent colonization of floral parts before harvest, a pattern also seen in other citrus fruit (Peever et al., 2004; Güney et al., 2023). While *G. citri-aurantii* showed intermediate aggressiveness, its threat is underscored by its unique thermal profile; its optimal growth at 30 °C makes it a significant concern for decay during transport or storage where temperatures may rise, a risk compounded by its known capacity for rapid spread and emerging fungicide resistance (Saito and Xiao, 2017; Nguyen et al., 2025). In contrast, the distinct preference of *P. expansum* for a cooler optimum of 20 °C shows that refrigeration does not eliminate risk, but rather shifts the competitive advantage to such cold-adapted species (Kanashiro et al., 2020). The low aggressiveness of *P. italicum* in our study, despite its broad optimal temperature range of 20–25 °C, suggests it may be a less dominant pathogen on kumquat compared to other citrus. This comprehensive temperature and virulence data has direct implications for managing the kumquat supply chain, highlighting the need for strict and uninterrupted temperature control to mitigate risks from both warm- and cool-adapted pathogens.

These findings show that an integrated, sustainable management approach is necessary, as traditional fungicides are increasingly limited by regulation, consumer demand for residue-free produce, and resistance development (Bhatta, 2022). Therefore, it is essential to explore and validate a combination of sustainable alternatives. These include non-chemical physical methods like plasma-activated water and UV light (Guo et al., 2021; Yang et al., 2022), natural preservatives such as essential oil vapors (Phala et al., 2022; Li et al., 2022), and the use of biocontrol agents like antagonistic yeasts and bacteria (Wang et al., 2022). Additionally, GRAS (Generally Recognized as Safe) salts like carbonates and bicarbonates are an effective and environmentally friendly control option (Palou et al., 2016; Türkkan et al., 2025a). Chloride-based salts, including calcium chloride ($CaCl_2$), potassium chloride (KCl), and sodium chloride (NaCl), are effective against *P. digitatum*, *P. italicum*, *P. expansum*, and *G. citri-aurantii*. Among these, $CaCl_2$ is particularly useful due to its dual action of inhibiting fungal growth while also reinforcing fruit tissues through calcium–pectate cross-linking (Türkkan et al., 2025b). An effective overall strategy will likely combine these treatments with packaging innovations, such as functionalized films or controlled-atmosphere storage (Zhang et al., 2022; Ashraf et al., 2025), to protect against the specific pathogens identified here.

This study identifies the primary fungi causing postharvest decay in kumquat as *A. alternata*, *G. citri-aurantii*, and three distinct *Penicillium* species. By fulfilling Koch's postulates and characterizing the aggressiveness and thermal biology of this pathogen complex, we have established the first complete pathogenic profile for this host, providing a critical baseline for all future research. The study's significance extends beyond this etiological breakthrough; we have also demonstrated the robust utility of a polyphasic approach, where high-throughput iPBS and SCoT fingerprinting serve as powerful, cost-effective tools for initial species delineation, validated by definitive multilocus phylogenetic analysis. This methodological framework offers a practical template for pathogen surveillance in other specialty fruit systems. Ultimately, these findings provide the essential scientific evidence needed to move from broad control tactics to targeted, evidence-based management strategies that can more effectively safeguard the quality and safety of kumquats in a growing global market.

CRediT authorship contribution statement

Mehtap Alkan: Resources, Investigation, Data curation, Methodology. **Göksel Özer**: Conceptualization, Writing – original draft, Writing – review & editing, Formal analysis, Funding acquisition. **Muharrem Türkkan**: Conceptualization, Writing – original draft, Writing – review & editing, Formal analysis, Funding acquisition. **Tuğba Bozoğlu**: Resources, Investigation, Data curation, Methodology. **İsmail Erper**: Resources, Conceptualization, Writing – review & editing. **Elif Yıldırım**: Resources, Investigation. **Davut Soner Akgül**: Resources, Conceptualization, Writing – review & editing. **T. Tarık Erper:** Resources, Investigation. **Rachid Lahlali**: Methodology, Formal analysis, Writing – review & editing. **Sibel Derviş**: Conceptualization, Writing – original draft, Writing – review & editing, Formal analysis, Funding acquisition.

Funding sources

This work was supported by The Scientific and Technological Research Council of Türkiye (TÜBİTAK) under project number 125O511.

Declaration of Competing Interest

The authors declare that they have no known competing financial interests or personal relationships that could have appeared to influence the work reported in this paper.

Acknowledgements

The authors would like to thank The Scientific and Technological Research Council of Türkiye (TÜBİTAK) for their financial support.

Data availability

The DNA sequence data generated during this study are publicly available in the NCBI GenBank database. Accession numbers are provided in Table 1 of the manuscript.

References

Ai, H., Zhang, Y., Reymick, O.O., Shen, X., Liu, W., Tao, N., Li, L., 2025. Extracellular polygalacturonase, β-1,4-glucanase, and β-xylosidase in *Geotrichum citri-aurantii* positively progressed the sour rot incidence in satsuma mandarin fruit. Postharvest Biol. Technol. 219, 113233. https://doi.org/10.1016/j.postharvbio.2024.113233.

Ashraf, M.A., Khan, A.S., Azam, M., 2025. Innovative technologies in postharvest management of fruits and vegetables: A review. Eur. Food Res. Technol. Advance online publication. https://doi.org/10.1007/s00217-025-04861-4.

Aydın, F., Özer, G., Alkan, M., Çakır, İ., 2020. The utility of iPBS retrotransposons markers to analyze genetic variation in yeast. Int. J. Food Microbiol. 325, 108647. https://doi.org/10.1016/j.ijfoodmicro.2020.108647.

Aydın, F., Özer, G., Alkan, M., Çakır, İ., 2022. Start codon targeted (SCoT) markers for the assessment of genetic diversity in yeast isolated from Turkish sourdough. Food Microbiol 107, 104081. https://doi.org/10.1016/j.fm.2022.104081.

Bhatta, U.K., 2022. Alternative management approaches of citrus diseases caused by *Penicillium digitatum* (green mold) and *Penicillium italicum* (blue mold). Front. Plant Sci. 12, 833328. https://doi.org/10.3389/fpls.2021.833328.

Chai, L., Xu, Q., Deng, C., Cheng, Y., Deng, X., 2022. New insights into the phylogeny and speciation of kumquat (*Fortunella* spp.) based on chloroplast SNP, nuclear SSR and whole-genome sequencing. Front. Agric. Sci. Eng. 9 (1), 36–50. https://doi.org/10.15302/J-FASE-2021436.

Chen, S., Jiang, W., Sun, Z., 2022. Mechanism of fungal inhibition activity of Nα-lauroyl-L-arginine ethyl ester (LAE) and potential in control of *Penicillium expansum* on postharvest citrus 'Benimadonna' (*Citrus reticulata* × *Citrus sinensis*). J. Sci. Food Agric. 102 (9), 3790–3799. https://doi.org/10.1002/jsfa.11827.

Cheng, Y., Lin, Y., Cao, H., Li, Z., 2020. Citrus postharvest green mold: Recent advances in fungal pathogenicity and fruit resistance. Microorganisms 8 (3), 449. https://doi.org/10.3390/microorganisms8030449.

Collard, B.C.Y., Mackill, D.J., 2009. Start codon targeted (SCoT) polymorphism: a simple, novel DNA marker technique for generating gene-targeted markers in plants. Plant Mol. Biol. Rep. 27, 86–93. https://doi.org/10.1007/s11105-008-0060-5.

Çakar, D., Özer, G., Akıllı Şimşek, S., Maden, S., 2023. Determination of vc and mating types of *Cryphonectria parasitica* isolates by multiplex PCR and their genetic diversity in 13 chestnut-growing provinces of Turkey. For. Pathol. 53 (3), e12813. https://doi.org/10.1111/efp.12813.

de Hoog, G.S., Smith, M.T., Guého, E., 1986. A revision of the genus *Geotrichum* and its teleomorphs. Stud. Mycol. 29, 1–60.

Fernandes, S.S., Peraza, C.C., Marasca, N.S., Egea, M.B., 2025. Effect of drying methods on the nutritional composition, technofunctional properties, and phytochemicals of kumquat (*Fortunella margarita*). J. Food Compos. Anal. 143, 107618. https://doi.org/10.1016/j.jfca.2025.107618.

Frisvad, J.C., Samson, R.A., 2004. Polyphasic taxonomy of *Penicillium* subgenus *Penicillium*: a guide to identification of food and air-borne terverticillate Penicillia and their mycotoxins. Stud. Mycol. 49, 1–174.

Guarnaccia, V., Crous, P.W., 2017. Species of *Diaporthe* on citrus in Europe. IMA Fungus 8 (2), 317–334. https://doi.org/10.5598/imafungus.2017.08.02.07.

Gui, Q., Zhao, J., Yu, Z., Sun, W., Mo, J., Li, Q., Hsiang, T., 2020. First report of trunk canker and gummosis of kumquat (*Fortunella margarita*) caused by *Lasiodiplodia theobromae* in mainland China. Plant Dis. 104 (5), 971. https://doi.org/10.1094/PDIS-02-19-0424-PDN.

Guo, J., Qin, D., Li, W., Wu, F., Li, L., Liu, X., 2021. Inactivation of *Penicillium italicum* on kumquat via plasma-activated water and its effects on quality attributes. Int. J. Food Microbiol 343, 109090. https://doi.org/10.1016/j.ijfoodmicro.2021.109090.

Gültekin, M.A., Özer, N., Özer, G., 2025. Molecular and pathogenic characterization of *Fusarium oxysporum* f. sp. *pisi* isolates obtained from Turkey. Eur. J. Plant Pathol. 171 (1), 37–52. https://doi.org/10.1007/s10658-024-02931-z.

Güney, İ.G., Tekin, F., Günen, T.U., Özer, G., Derviş, S., 2023. *Alternaria alternata* causing inner black rot of lemon (*Citrus limon*) fruits in Turkey: genetic diversity and characterisation. Physiol. Mol. Plant Pathol. 125, 101998. https://doi.org/10.1016/j.pmpp.2023.101998.

Houbraken, J., Wang, L., Lee, H.B., Frisvad, J.C., 2016. New sections in *Penicillium* containing novel species producing patulin, pyripyropens or other bioactive compounds. Pers. Mol. Phylogeny Evol. Fungi 36 (1), 299–314. https://doi.org/10.3767/003158516X692040.

Jung, T., Orlikowski, L., Henricot, B., Abad-Campos, P., Aday, A.G., Aguín Casal, O., Pérez-Sierra, A., 2016. Widespread *Phytophthora infestations* in European nurseries put forest, semi-natural and horticultural ecosystems at high risk of Phytophthora diseases. For. Pathol. 46 (2), 134–163. https://doi.org/10.1111/efp.12239.

Kalendar, R., Antonius, K., Smýkal, P., Schulman, A.H., 2010. iPBS: a universal method for DNA fingerprinting and retrotransposon isolation. Theor. Appl. Genet 121 (8), 1419–1430. https://doi.org/10.1007/s00122-010-1398-2.

Kanashiro, A.M., Akiyama, D.Y., Kupper, K.C., Fill, T.P., 2020. *Penicillium italicum*: an underexplored postharvest pathogen. Front. Microbiol. 11, 606852. https://doi.org/10.3389/fmicb.2020.606852.

Kumar, S., Stecher, G., Li, M., Knyaz, C., Tamura, K., 2018. MEGA X: molecular evolutionary genetics analysis across computing platforms. Mol. Biol. Evol. 35 (6), 1547–1549. https://doi.org/10.1093/molbev/msy096.

Kurbetli, İ., Sülü, G., Aydoğdu, M., Özdemir, M., Sülü, S.M., Polat, İ., 2016. First report of kumquat shoot blight caused by *Phytophthora citrophthora* in Turkey. Plant Dis. 100 (5), 1023. https://doi.org/10.1094/PDIS-10-15-1154-PDN.

Laurin, E., Nunes, M.C.N., Émond, J.P., 2005. Re-cooling of strawberries after air shipment delays fruit senescence. Acta Hortic. (682), 1745–1752. https://doi.org/10.17660/ActaHortic.2005.682.233.

Leonardi, G.R., Aiello, D., Camilleri, G., Piattino, V., Polizzi, G., Guarnaccia, V., 2023. A new disease of kumquat (*Fortunella margarita*) caused by *Colletotrichum karsti*: twig and branch dieback. Phytopathol. Mediterr. 62 (3), 333–348. https://doi.org/10.36253/phyto-14231.

Li, M., Wang, M., Hu, S., Sun, J., Zhu, M., Ni, Y., Wang, J., 2022. Advanced coatings with antioxidant and antibacterial activity for kumquat preservation. Foods 11 (15), 2363. https://doi.org/10.3390/foods11152363.

Liu, Y.M., Liu, Y., Liu, Y.M., Liu, H.D., Shang, Y.S., 2018. Evaluating effects of ellagic acid on the quality of kumquat fruits during storage. Sci. Hortic. 227, 244–254. https://doi.org/10.1016/j.scienta.2017.08.055.

Ma, Q.L., Hu, Y.W., Dong, X.H., Zhou, G.F., Liu, X., Gu, Q.Q., Wei, Q.J., 2021. Metabolic profiling and gene expression analysis unveil differences in flavonoid and lipid metabolisms between 'Huapi' kumquat (*Fortunella crassifolia* Swingle) and its wild type. Front. Plant Sci. 12, 759968. https://doi.org/10.3389/fpls.2021.759968.

Miller, M.A., Pfeiffer, W., Schwartz, T., 2011. The CIPRES science gateway: a community resource for phylogenetic analyses. Proceedings of the 2011 TeraGrid Conference: extreme digital discovery 1–8. https://doi.org/10.1145/2016741.2016785.

Muratali, D., Derviş, S., Özer, G., 2025. Molecular and pathogenic characterization of *Fusarium* species associated with dry rot in stored potatoes in Kyrgyzstan. Potato Res. https://doi.org/10.1007/s11540-025-09872-y.

Nguyen, A.M., Foerster, H., Adaskaveg, J.E., 2025. Identification of *Geotrichum citri-aurantii* and *G. candidum* in citrus packinghouses in California, their sensitivity to cyproconazole, and incomplete cross-resistance to propiconazole. Plant Dis. 109 (4), 825–833. https://doi.org/10.1094/PDIS-08-24-1692-RE.

Palacıoğlu, G., Alkan, M., Derviş, S., Bayraktar, H., Özer, G., 2023. Molecular phylogeny of plant pathogenic fungi based on start codon targeted (SCoT) polymorphism. Mol. Biol. Rep. 50 (10), 8271–8279. https://doi.org/10.1007/s11033-023-08735-4.

Palou, L., Ali, A., Fallik, E., Romanazzi, G., 2016. GRAS, plant- and animal-derived compounds as alternatives to conventional fungicides for the control of postharvest diseases of fresh horticultural produce. Postharvest Biol. Technol. 122, 41–52. https://doi.org/10.1016/j.postharvbio.2016.04.017.

Pawełczyk, A., Żwawiak, J., Zaprutko, L., 2023. Kumquat fruits as an important source of food ingredients and utility compounds. Food Rev. Int. 39 (2), 875–895. https://doi.org/10.1080/87559129.2021.1928179.

Peever, T.L., Su, G., Carpenter-Boggs, L., Timmer, L.W., 2004. Molecular systematics of citrus-associated *Alternaria* species. Mycologia 96 (1), 119–134. https://doi.org/10.2307/3761993.

Phala, K., Augustyn, W., Combrinck, S., Botha, B., Regnier, T., Du Plooy, W., 2022. Inhibition of kumquat postharvest fungi through vapor contact with spearmint essential oil and carvone. ACS Agric. Sci. Technol. 2(2), 330–339. ⟨https://orcid.org/0000-0003-2463-5142⟩.

Plaza, P., Usall, J., Teixidó, N., Viñas, I., 2003. Effect of water activity and temperature on germination and growth of *Penicillium digitatum*, *P. italicum* and *Geotrichum candidum*. J. Appl. Microbiol. 94 (4), 549–554. https://doi.org/10.1046/j.1365-2672.2003.01909.x.

Rohlf, F.J., 2000. NTSYS-pc: numerical taxonomy and multivariate analysis system, version 2.1. New York. Exeter Software.

Saito, S., Xiao, C.L., 2017. Prevalence of postharvest diseases of mandarin fruit in California. Plant Health Prog. 18 (4), 204–210. https://doi.org/10.1094/PHP-07-17-0041-RS.

Schirra, M., Angloni, A., Cabras, P., D'Aquino, S., Palma, A., 2011. Effects of postharvest hot water and hot air treatments on storage decay and quality traits of kumquat (*Fortunella japonica* Lour. Swingle, cv. Ovale) fruit. J. Agric. Sci. Technol. B 1, 89–94. https://doi.org/10.1007/s10709-007-9196-8.

Simmons, E.G., 2007. Alternaria: An Identification Manual. CBS Fungal Biodiversity Center, Utrecht, The Netherlands.

Tekin, F., Altın, İ., Aydın, F., Alkan, M., Canik Orel, D., Ardıç, M., Gašić, K., Kovács, T., Allen, C., Özer, G., 2024. Unveiling genetic diversity among bacterial isolates using SCoT markers. Curr. Microbiol. 81, 409. https://doi.org/10.1007/s00284-024-03938-9.

Thompson, J.F., Slaughter, D.C., Arpaia, M.L., 2008. Suspended tray package for protecting soft fruit from mechanical damage. Appl. Eng. Agric. 24 (1), 71–75. https://doi.org/10.13031/2013.24149.

Türkkan, M., Bozoğlu, T., Derviş, S., Özer, G., Erper, İ., 2024. *Armillaria* species causing kiwifruit vine decline and root rot in Northeastern Türkiye: a growing concern for kiwifruit health. J. Phytopathol. 172 (5), e13409. https://doi.org/10.1111/jph.13409.

Türkkan, M., Özer, G., Taheri, P., Derviş, S., 2025a. Carbonates and bicarbonates: a sustainable approach for managing plant diseases, pests, and abiotic stresses. Physiol. Mol. Plant Pathol. 139, 102795. https://doi.org/10.1016/j.pmpp.2025.102795.

Türkkan, M., Özer, G., Taheri, P., Derviş, S., 2025b. Sustainable use of chlorides against biotic and abiotic stresses. Environmentally safe strategies for plant protection against biotic and abiotic stresses. Elsevier, pp. 329–383. https://doi.org/10.1016/B978-0-443-23818-5.00017-X.

Wang, Z., Sui, Y., Li, J., Tian, X., Wang, Q., 2022. Biological control of postharvest fungal decays in citrus: a review. Crit. Rev. Food Sci. Nutr. 62 (4), 861–870. https://doi.org/10.1080/10408398.2020.1829542.

Woudenberg, J.H.C., Seidl, M.F., Groenewald, J.Z., de Vries, M., Stielow, J.B., Thomma, B.P., Crous, P.W., 2015. *Alternaria* section *Alternaria*: species, formae speciales or pathotypes? Stud. Mycol. 82 (1), 1–21. https://doi.org/10.1016/j.simyco.2015.07.001.

Wu, G.A., Terol, J., Ibanez, V., López-García, A., Pérez-Román, E., Borredá, C., Domingo, C., Tadeo, F.R., Carbonell-Caballero, J., Alonso, R., 2018. Genomics of the origin and evolution of Citrus. Nature 554 (7692), 311–316. https://doi.org/10.1038/nature25447.

Yang, L., Qiu, L., Liu, D., Kuang, L., Hu, W., Liu, Y., 2022. Changes in the crystal morphology, chemical composition and key gene expression of 'Suichuan' kumquat cuticular waxes after hot water dipping. Sci. Hortic. 293, 110753. https://doi.org/10.1016/j.scienta.2021.110753.

Yang, L., Hu, W., Liu, D., Qiu, L., Kuang, L., Song, J., Huang, Y., Xie, J., Liu, Y., 2023. Comparative analysis of the crystal morphology, chemical composition and key gene expression between two kumquat fruit cuticular waxes during postharvest cold storage. Postharvest Biol. Technol. 206, 112550. https://doi.org/10.1016/j.postharvbio.2023.112550.

Zhang, L., Wang, W., Ni, Y., Yang, C., Jin, X., Wang, Y., Wang, J., 2022. ZnO/C-mediated k-carrageenan based pseudo-pasteurization films for kumquat preservation. Food Hydrocoll. 128, 107582.

Zhu, L., Chen, G.Q., Zhao, X.L., Deng, C.L., Hyde, K.D., Li, H.Y., 2013. *Fusarium* spp. are responsible for shoot canker of kumquat in China. J. Phytopathol. 161 (1), 59–62. https://doi.org/10.1111/jph.12019.

Zhu, M., Wang, Y., Zeng, Z., Wu, X., Teng, J., Zhang, J., Atkinson, R.G., 2024. A natural mutant kumquat fruit with abnormal oil glands shows lower volatile production, better fruit flavor and higher resistance to postharvest disease. Postharvest Biol. Technol. 210, 112739. https://doi.org/10.1016/j.postharvbio.2023.112739.